Silicon (2018) 10:2617–2625
https://doi.org/10.1007/s12633-018-9798-z

ORIGINAL PAPER

Simultaneous Prediction of the Density, Viscosity and Electrical Conductivity of Pyridinium-Based Hydrophobic Ionic Liquids Using Artificial Neural Network

Ehsan Kianfar[1] · Maryam Shirshahi[2] · Farangis Kianfar[3] · Farshid Kianfar[4]

Received: 15 August 2017 / Accepted: 1 March 2018 / Published online: 12 April 2018

Abstract
An Artificial Neural Network (ANN) model is presented for the Simultaneous prediction of density, viscosity and electrical conductivity of pyridinium-based hydrophobic ionic liquids. Data density, viscosity and electrical conductivity obtained from paper and from a three layer feed forward artificial neural network is used to estimate them. The optimal ANN model consisted of, two neurons in the input layer, ten neurons in the hidden layer and three neurons in the output layer. This model predicts the density with a Mean Square Error (MSE) of 7.5714×10^{-7} and the coefficient of determination (R^2) of 1.0000, viscosity with a Mean Square Error (MSE) of 1.1332×10^{-4} and the coefficient of determination (R^2) of 0.9982 and electrical conductivity with a Mean Square Error (MSE) of 2.2668×10^{-6} and the coefficient of determination (R^2) of 0.9999. The results show that the Simultaneous predicted of density, viscosity and electrical conductivity of pyridinium-based hydrophobic ionic liquids by using artificial neural network well done. The artificial neural network model shows lower errors and higher precision compared to statistical models while use of ANN is easier and quicker than statistical methods.

Keywords Density · Viscosity · Electrical conductivity · Artificial neural network · Ionic liquids

1 Introduction

Recently, the ionic liquids have been considerably paid into attention by the researchers due to their unique properties. Although determination of thermodynamic properties is of high importance due to be used in industry, achievement of such data is costly and time-wasting. Despite wide technological advances, most of analytical devices cannot directly analyze slight amount of analyte in actual samples (complex tissues) [1]. Therefore, in order to solve this problem, those preparation steps are taken before analysis that in addition to separation of species from their complex matrix, they can concurrently provide analyte concentration, as well. Therefore, analyte may be measured even in very low concentrations. Liquid-liquid extraction is a classic preparation approach used in most of standard methods. Despite wide applications and popularity, it has such defects as formation of emulsion, time-wasting and tiring. Consequently, it is classified as multistage preparation method which requires high volumes of expensive and toxic organic solvents which may cause serious damages for human health and environment. Solid phase extraction is another classic preparation method. Although this method needs less organic solvent compared to the former, it suffers time-wasting, high cost, low repeatability and high usage of organic solvent [2]. Looking for new preparation methods never has been interrupted. For this reason, plenty of studies are conducted for the separation associated with modern techniques of sample preparation which provides such advantages as high speed, simplicity and high efficiency and has been successfully able to overcome the problem of use of organic solvents. The ionic liquids are the

✉ Ehsan Kianfar
e-kianfar94@iau-arak.ac.ir; Ehsan_kianfar2010@yahoo.com

1 Department of Chemical Engineering, Arak Branch, Islamic Azad University, Arak, Iran

2 Department of Civil Engineering, Arak Branch, Islamic Azad University, Arak, Iran

3 Department of Chemistry, Gachsaran Branch, Islamic Azad University, Gachsaran, Iran

4 Department of Chemical Engineering, North Tehran Branch, Islamic Azad University, North Tehran, Iran

compositions which have revolutionized chemical industries and the corresponding researches. They are considered as green chemicals which play a very important role as a solvent to reduce use of hazardous, toxic and harmful compounds for the environment. The ionic liquids can be an alternative for plenty of conventional solvents in pharmaceuticals. Nowadays, the ionic liquids are accounted for the organic compounds formed by ions and be liquid in a temperature of 100 °C. One of the reasons of increased studies on ionic liquids is the goal of scientists to look for a suitable alternative for volatile organic solvents among the industries. Volatile organic solvents are the known as the most important resource of environmental pollution in chemical and pharmaceutical industries [3–5]. However, this does not mean that the ionic liquids are entirely considered as green solvents, some of them are even substantially toxic. There are diverse types of ionic liquids including those in the room temperature, chiral ionic liquids, hydrophobic ionic liquids, and so on. The former are those being liquefied at the room temperature with a wide application in ionic liquids chemistry. The extensive use of toxic and volatile solvents in chemical industries may cause to seriously damage the environment. Therefore, it makes sense among pharmaceutical and chemical industries to find a suitable alternative for such solvents which are environmentally proper and have conventional solvents properties. Supercritical carbon dioxide and ionic liquids are of the new solvents well-known as the green catalysts. The ionic liquids contain some organic compounds which are wholly composed of ions. These compounds are usually liquid at the temperatures under 100 °C, while lack of considerable vapor pressure is their most important advantage and for this reason, it is volatile and makes no problem for the environment [6–9]. Molecular structure of ionic liquids consists of diverse Cations and Anions. The role of Cation is typically played by a bulky organic compound (positively charged) while the latter has an inorganic structure and is far smaller than the former in terms of size (negatively charged). Due to different size of Anions and Cations, the bond between these two components of ionic liquids is poor while such compounds are liquid-formed at the temperatures under 100 °C. The structure of ionic liquid is same as that of sodium chloride but the latter has a strong crystal structure and is molten in a temperature of 800 °C due to strong bond between Cation and Anion (high similarity of Cations and Anions in terms of size, load and nature) [10–13]. The temperature of 100 °C is considered for classification of ionic liquids: those being liquid at the temperatures above 100 °C are known as molten liquid and those having liquid mode at a temperature under 100 °C are called ionic liquids. There exist two major group of ionic liquid including the compounds which are respectively made of organic molecules of Imidazolium (Imidazole compound with $C_3H_4N_2$ formulation) and Pyridinium (Pyridinium compound with C_5H_5N formula) as Cation. The structures of both groups are shown in Fig. 1. Diverse Cations and Anions are used to prepare ionic liquids, making ionic liquids with dedicated uses or strengthened physico-chemical properties. The conventional Anions include BF^4, BF^6, Br^-, Cl^-, etc. [14].

2 Methodology

2.1 Collecting Density, Viscosity and Electrical Conductivity of Pyridinium-Based Ionic Liquids

The required data was found from the paper with temperature-based density, viscosity and electrical conductivity amounts Table 1 [15].

2.2 Educational (Trainings) Process for Artificial Neural Networks

The success in artificial neural network modeling depends on two factors: 1- quantity of data, 2-data distribution at tests conducting range [16]. In case of large databases and similar training models, the educational/training process will be disrupted. Hence, it makes sense to design tests to disperse pattern among necessary independent value ranges. In order to review and evaluate diverse networks, the databases are divided into two groups: 1- Training, 2- Test. It is noteworthy to mention that assessment models are used to review generalization performance of the used networks, while general patterns are employed to prevent Over Training. Selection of network architecture is the first step to create artificial neural networks after which the networks trainings are conducted using the input-output models made in the test such that artificial neural networks will learn the relation between neurons at every training cycle using training data during the training, approaching predicted values to suitable output data and lowering the specified error values. The combinational parameters (e.g. hidden layers, number of neurons, number of training cycles, learning rate and momentum) are specified within the neural network training process by trial and error method. The generalization capability of the trained neural network is the last step in development of artificial neural network model. In this step, the trained neural network models are tested through assessment data sets which are independent from training data. In order to find a network with a suitable architecture using training models, mean squared error benchmark is used which is defined by Eq. 1. E_{RMS} It is accounted for the primary benchmark for selection of suitable architecture [17] Where, E_{RMS} is the mean square error at training step, S_{ip} is the network output in i^{th} neuron and p^{th} model, Tip is the target output at i^{th} neuron and p^{th} model, n_p is the

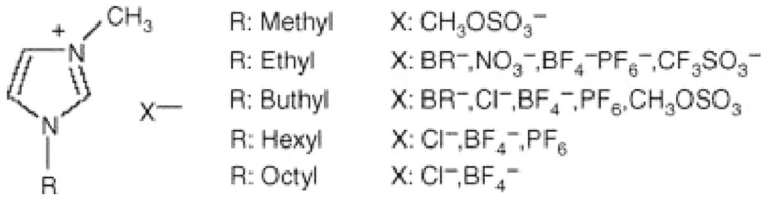

(a) Imidazolium

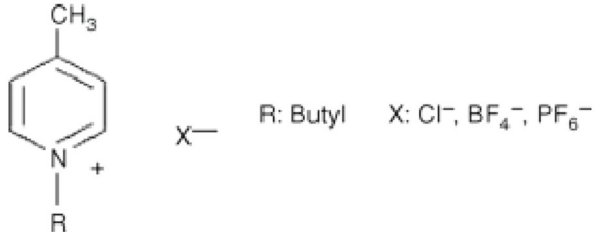

(b) Pyridinium

Fig. 1 Ionic liquids Cation with **a** Imidazolium **b** pyridine [14]

number of models, n_o is the number of neurons of output layer, N is number of output neurons and M is number of training models. The objective is to minimize errors. Several benchmarks were used to assess artificial networks learning as self-training generalization to reach the best possible results. The statistical values to assess generalizability include coefficient of determination (R^2), mean absolute error (E_{ma}), standard deviation of mean absolute error (SD_{ma}), mean relative error (E_{mr}), standard deviation of mean relative error (SD_{mr}) which are respectively calculated by the following equations:

$$E_{RMS} = \frac{\sqrt{\sum_{p=1}^{M}\sum_{i=1}^{N}(S_{ip} - T_{ip})^2}}{n_p \times n_o} \quad (1)$$

$$T_m = \left(\frac{\sum_{k=1}^{n} S_k}{n}\right) \quad (2)$$

Table 1 Density, viscosity and electrical conductivity values of Pyridinium-based ionic liquids [15]

T(°K)	$[C_3 3mpy][ntf_2]$			$[C_6 3mpy][ntf_2]$			$[C_6 4mpy][ntf_2]$		
	Density ($g.cm^{-3}$)	Viscosity (mpa.s)	Electrical conductivity ($mS.cm^{-1}$)	Density ($g.cm^{-3}$)	Viscosity (mpa.s)	Electrical conductivity ($mS.cm^{-1}$)	Density ($g.cm^{-3}$)	Viscosity (mpa.s)	Electrical conductivity ($mS.cm^{-1}$)
278.15	1.4685[a]	160.80[a]	1.524	1.3781[a]	276.16[a]	0.495	1.3695[a]	253.47[a]	0.592[a]
283.15	1.4640[a]	118.12[a]	1.990	1.3736	199.61[a]	0.670	1.3653	181.62	0.839
288.15	1.4596	89.08[a]	2.53	1.3697	147.89[a]	0.885	1.3608	133.92	1.101
293.15	1.4556	68.73[a]	3.18	1.3653	112.00[a]	1.157	1.3563	101.07	1.447
298.15	1.4514	54.12	3.93	1.3615	86.59	1.480	1.3518	77.989	1.852
303.15	1.4380	43.46	4.76	1.3570	67.83	1.869	1.3474	61.301	2.31
308.15	1.4426	35.27	5.71	1.3529	54.23	2.31	1.3429	49.031	2.83
313.15	1.4380	29.18	6.71	1.3487	44.24	2.83	1.3385	39.755	3.46
318.15	1.4332	24.32	7.86	1.3447	36.21	3.42	1.3341	32.729	4.15
323.15	1.4245	20.87	9.04	1.3403	29.97	4.06	1.3296	27.381	4.87
328.15	1.4287	17.94	10.36	1.3360	25.08	4.77	1.3252	23.111	5.71
333.15	1.4245	15.15	11.79	1.3317	21.31	5.53	1.3208	19.709	6.52
338.15	1.4160	13.40	13.29	1.3280	18.28	6.38	1.3165	16.968	7.56
343.15	1.4113[a]	11.74	14.85	1.3237[a]	15.88	7.28	1.3121	14.729	8.61
348.15	1.4069[a]	10.37	16.50	1.3195[a]	13.71	8.22	1.3078	12.866	9.68
353.15	1.4025[a]	9.19	18.29	1.3154[a]	11.99	9.20	1.3034	11.324	10.75

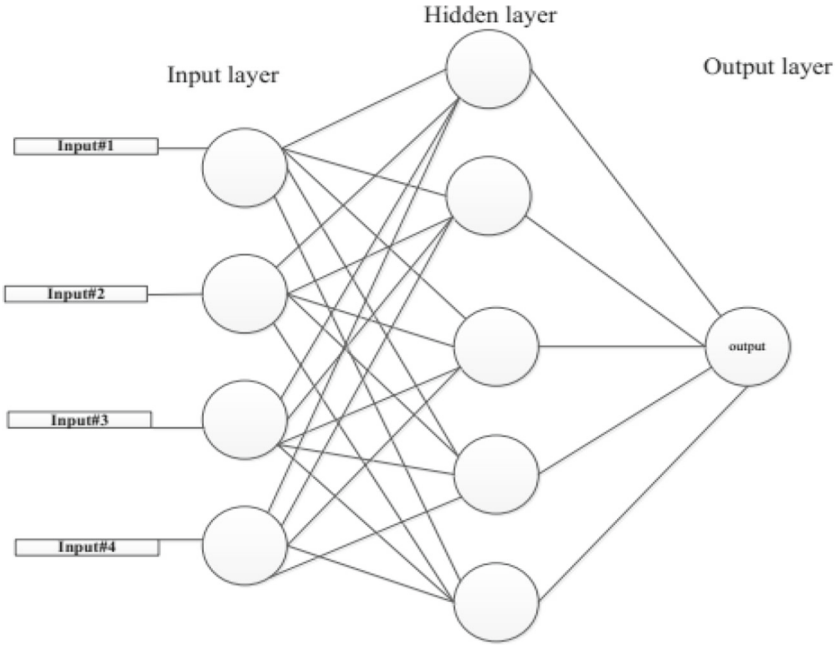

Fig. 2 Structure of artificial neural network

$$R^2 = 1 - \left(\sum_{k=1}^{n} [S_k - T_k] / \sum_{k=1}^{n} [S_k - T_m]\right) \quad (3)$$

$$E_{ma} = \frac{1}{n}\sum_{k-1}^{n} |S_k - T_k| \quad (4)$$

$$SD_{ma} = \sqrt{\frac{\sum_{k=1}^{n}(|S_k - T_k| - |\overline{S_k - T_k}|)}{n-1}} \quad (5)$$

$$E_{mr} = \frac{1}{n}\sum_{k=1}^{n} \left|\frac{S_k - T_k}{T_k}\right| \quad (6)$$

Table 2 Statistical results for prediction of density by diverse topologies of artificial neural network

Neuron	Density					
	Education		Test		Total	
	MSE	R^2	MSE	R^2	MSE	R^2
1	0.0109	0.8144	0.0127	0.7165	0.0114	0.7971
2	$2.9841*10^{-4}$	0.9949	$4.8736*10^{-4}$	0.9891	$3.4565*10^{-4}$	0.9938
3	$2.7448*10^{-4}$	0.9953	$3.3077*10^{-4}$	0.9926	$2.8855*10^{-4}$	0.9948
4	$3.4551*10^{-5}$	0.9994	$7.5810*10^{-5}$	0.9983	$4.4683*10^{-5}$	0.9992
5	$2.0441*10^{-5}$	0.9997	$8.2832*10^{-5}$	0.9981	$3.6039*10^{-5}$	0.9994
6	$1.5606*10^{-5}$	0.9997	$2.4708*10^{-5}$	0.9994	$1.7881*10^{-5}$	0.9997
7	$1.0381*10^{-5}$	0.9998	$1.3268*10^{-4}$	0.9970	$4.0957*10^{-5}$	0.9993
8	$5.1069*10^{-7}$	1.0000	$8.3581*10^{-7}$	1.0000	$5.9197*10^{-6}$	1.0000
9	$1.1946*10^{-6}$	1.0000	$3.2968*10^{-6}$	0.9999	$1.7202*10^{-6}$	1.0000
10	$3.6487*10^{-7}$	1.0000	$7.5714*10^{-7}$	1.0000	$4.6294*10^{-7}$	1.0000
11	$5.3694*10^{-7}$	1.0000	$1.4119*10^{-6}$	1.0000	$7.5748*10^{-7}$	1.0000
12	$2.3138*10^{-7}$	1.0000	$1.1453*10^{-4}$	0.9974	$2.8805*10^{-5}$	0.9995
13	$2.4441*10^{-7}$	1.0000	$4.6038*10^{-6}$	0.9999	$1.3343*10^{-6}$	1.0000
14	$1.6284*10^{-7}$	1.0000	0.0014	0.9687	$3.4960*10^{-4}$	0.9938
15	$2.0278*10^{-7}$	1.0000	$2.4929*10^{-4}$	0.9944	$6.2475*10^{-5}$	0.9989
20	$9.1050*10^{-8}$	1.0000	0.0062	0.8603	0.0016	0.9811
25	$1.0714*10^{-7}$	1.0000	0.0038	0.9141	$9.5839*10^{-4}$	0.9829
30	$1.1615*10^{-8}$	1.0000	$2.0058*10^{-4}$	0.9955	$5.0153*10^{-5}$	0.9991
35	$3.0659*10^{-12}$	1.0000	$3.2750*10^{-4}$	0.9927	$8.1875*10^{-5}$	0.9985

Table 3 Statistical results for prediction of viscosity by diverse topologies of artificial neural network

Neuron	Viscosity					
	Education		Test		Total	
	MSE	R^2	MSE	R^2	MSE	R^2
1	0.0244	0.0361	0.0703	0.1461	0.0359	0.0212
2	0.0062	0.7569	0.0184	0.7004	0.0092	0.7487
3	$5.3802*10^{-4}$	0.9787	0.0053	0.9135	0.0017	0.9528
4	$2.0126*10^{-4}$	0.9920	0.0026	0.9582	$7.9234*10^{-4}$	0.9784
5	$5.6695*10^{-6}$	0.9998	$3.9307*10^{-4}$	0.9936	$1.0252*10^{-4}$	0.9972
6	$7.9203*10^{-6}$	0.9997	$2.0410*10^{-5}$	0.9997	$1.1118*10^{-5}$	0.9997
7	$2.3310*10^{-6}$	0.9999	$6.9204*10^{-4}$	0.9887	$1.7431*10^{-4}$	0.9952
8	$7.2417*10^{-7}$	1.0000	$1.5820*10^{-4}$	0.9974	$4.0092*10^{-5}$	0.9989
9	$9.6851*10^{-7}$	1.0000	$2.2158*10^{-5}$	0.9996	$6.2658*10^{-5}$	0.9998
10	$1.2203*10^{-7}$	1.0000	$1.1332*10^{-4}$	0.9982	$2.8420*10^{-5}$	0.9992
11	$7.4653*10^{-7}$	1.0000	$2.9658*10^{-4}$	0.9952	$7.4705*10^{-5}$	0.9980
12	$1.7274*10^{-7}$	1.0000	0.0027	0.9568	$6.6315*10^{-4}$	0.9819
13	$3.3507*10^{-8}$	1.0000	$2.5893*10^{-6}$	1.0000	$6.7246*10^{-7}$	1.0000
14	$3.0658*10^{-7}$	1.0000	0.0013	0.9795	$3.1532*10^{*-4}$	0.9914
15	$5.6451*10^{-8}$	1.0000	$1.6681*10^{-4}$	0.9973	$4.1745*10^{-4}$	0.9989
20	$1.3446*10^{-8}$	1.0000	0.0030	0.9503	$7.6248*10^{-4}$	0.9792
25	$1.9718*10^{-8}$	1.0000	0.0131	0.7864	0.0033	0.9106
30	$5.8880*10^{-10}$	1.0000	0.0269	0.5623	0.0067	0.8168
35	$3.8363*10^{-12}$	1.0000	$9.5502*10^{-4}$	0.9844	$2.3875*10^{-4}$	0.9935

Table 4 Statistical results for prediction of electrical conductivity by diverse topologies of artificial neural network

Neuron	Electrical conductivity					
	Education		Test		Total	
	MSE	R^2	MSE	R^2	MSE	R^2
1	0.0309	0.2601	0.0250	0.2888	0.0294	0.2303
2	0.0032	0.9228	0.0051	0.7371	0.0037	0.9034
3	0.0011	0.9746	0.0011	0.9456	0.0011	0.9723
4	$4.2677*10^{-5}$	0.9990	$3.9870*10^{-5}$	0.9979	$4.1975*10^{-5}$	0.9989
5	$9.5321*10^{-6}$	0.9980	$7.6040*10^{-5}$	0.9961	$2.6159*10^{-5}$	0.9993
6	$5.6413*10^{-6}$	0.9999	$4.5134*10^{-5}$	0.9977	$1.5515*10^{-5}$	0.9996
7	$3.9581*10^{-6}$	0.9999	$5.2904*10^{-6}$	0.9997	$4.0957*10^{-5}$	0.9999
8	$4.9595*10^{-7}$	1.0000	$2.8902*10^{-6}$	0.9999	$1.0945*10^{-6}$	1.0000
9	$7.2414*10^{-7}$	1.0000	$2.7166*10^{-6}$	0.9999	$1.2223*10^{-6}$	1.0000
10	$4.9843*10^{-7}$	1.0000	$2.2668*10^{-8}$	0.9999	$9.4053*10^{-7}$	1.0000
11	$6.3304*10^{-7}$	1.0000	$2.1833*10^{-6}$	0.9999	$1.0206*10^{-6}$	1.0000
12	$1.5332*10^{-7}$	1.0000	$3.2730*10^{-6}$	0.9983	$8.2976*10^{-6}$	0.9998
13	$1.5451*10^{-7}$	1.0000	$4.4850*10^{-6}$	0.9998	$1.2371*10^{-6}$	1.0000
14	$5.7224*10^{-7}$	1.0000	$1.1423*10^{-5}$	0.9994	$3.2848*10^{-6}$	0.9999
15	$1.1190*10^{-7}$	1.0000	$7.7810*10^{-4}$	0.9599	$1.9461*10^{-4}$	0.9949
20	$2.2738*10^{-8}$	1.0000	0.0029	0.8511	$7.2201*10^{-4}$	0.9722
25	$2.0521*10^{-8}$	1.0000	0.0046	0.7611	0.0012	0.9697
30	$1.1667*10^{-11}$	1.0000	0.0028	0.8571	$6.9254*10^{-4}$	0.9819
35	$3.8195*10^{-12}$	1.0000	$4.5292*10^{-4}$	0.9766	$1.1323*10^{-4}$	0.9970

$$SD_{mr} = \sqrt{\frac{\sum_{k=1}^{n}\left(\left|\frac{S_k - T_k}{T_k}\right| - \left|\frac{\overline{S_k - T_k}}{T_k}\right|\right)}{n-1}} \quad (7)$$

In these equations, S_k is the predicted value by artificial neural network for the k^{th} model, T_k is the target value (trail value) for the k^{th} model, T_m is the mean predicted values and n is number of training models. In this paper, the software package MATLAB version 7 was used to create multilayer feedforward neural network for simulation. This type of neural network is actually a strong and optimal model for simulation [18]. In present study, a three-layer feedforward topology was used with 2 neurons in input layer, 10 neurons in hidden layer and 3 neurons in external layer which are shown in Fig. 2. A propagation algorithm was employed for the training under supervision of such topologies, a sigmoid transfer function was used for the hidden layer and a linear transfer function was hired for the external layer. The weights and biases were selected randomly at the beginning of training. The inputs included normalized temperature while density, viscosity and electrical conductivity were considered as outputs. Number of neurons in the hidden layer was varied at ranges of 1–15 (one-by-one) and 15–35 (five-by-five). The training was assessed to find the best topology with such number of neurons and the least errors at the hidden layer. In order to prevent Over Training, the propagation algorithm was used by two methods: A) early stopping and B) the least number of neurons at hidden layer [18]. As mentioned above, the available data is divided into three groups which were used for network training, network assessment while training and testing the network, respectively. A number of 1000 cycles was applied while training and networks testing.

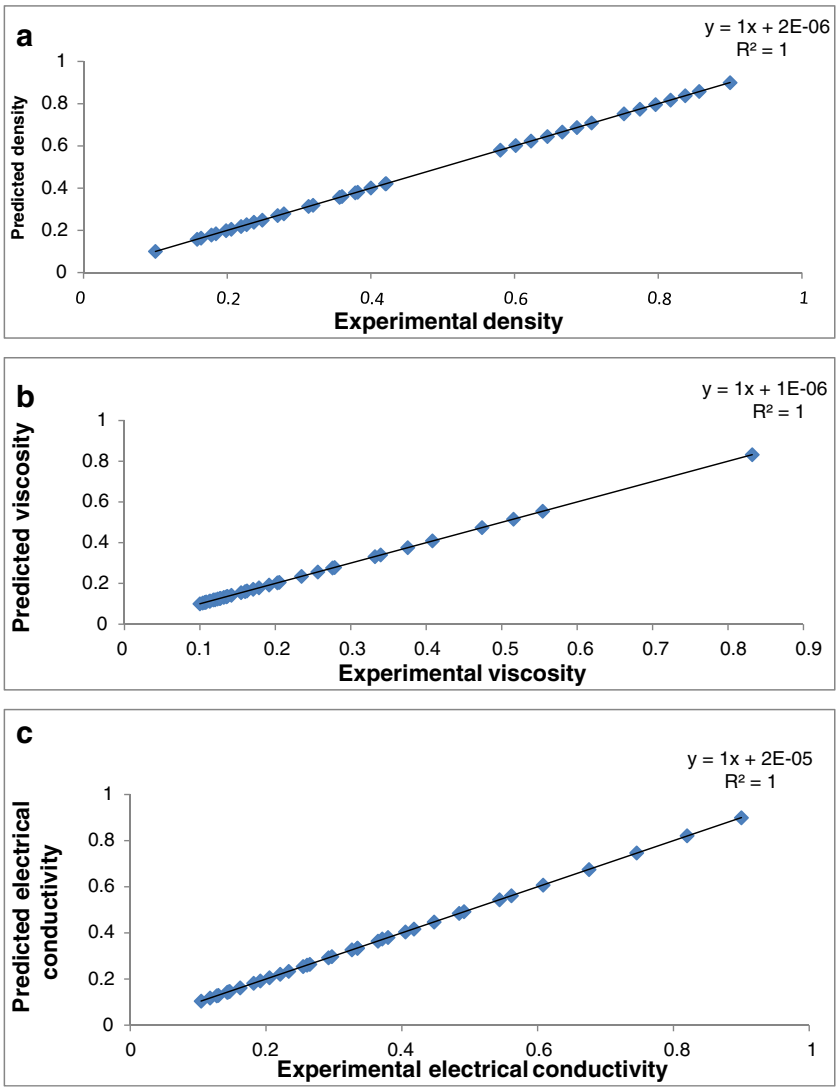

Fig. 3 The predicted values of normalized versus experimental data for **a** density **b** viscosity **c** electrical conductivity and testing set using the ANN model

2.3 Selection of Optimal Artificial Neural Network (ANN) Topology

The comparison of mean squared error (MSE) and linear regression factor (R^2) between experimental and predicted values by ANN topology and Sum Squared Error (SSE) and Root Mean Squared Error (RMSE) was used here to predict performance of ANN topology. The measured errors and coefficient of determination are respectively calculated by following equations:

$$\mathrm{MSE} = \frac{1}{N}\sum_{i=1}^{N}(|y_i - y_{id}|)^2 \tag{8}$$

$$\mathrm{RMSE} = \frac{1}{N}\sum_{i=1}^{N}\left(\left|\frac{y_i - y_{id}}{y_{id}}\right|\right)^2 \tag{9}$$

$$\mathrm{SSE} = \sum_{i=1}^{N}(y_i - y_{id})^2 \tag{10}$$

$$R^2 = 1 - \frac{\sum_{i=1}^{N}(y_i - y_{id})}{\sum_{i=1}^{N}(y_i - y_m)} \tag{11}$$

where y_i is the predicted value by ANN topology, y_{id} is the experimental value, y_m is the mean experimental value is N is the number of data.

3 Results and Discussion

In this paper, a number of 48 derived data for density, viscosity and electrical conductivity is divided into two groups: 1. Including 36 data for the network training and, 2. 12 data for testing the neural network and obtaining final results. Several ANN topologies were assessed to reach desired model. At every step, Mean Squared Error (MSE) and coefficient of determination (R^2) were calculated, which are presented in Tables 2, 3 and 4 regarding diverse

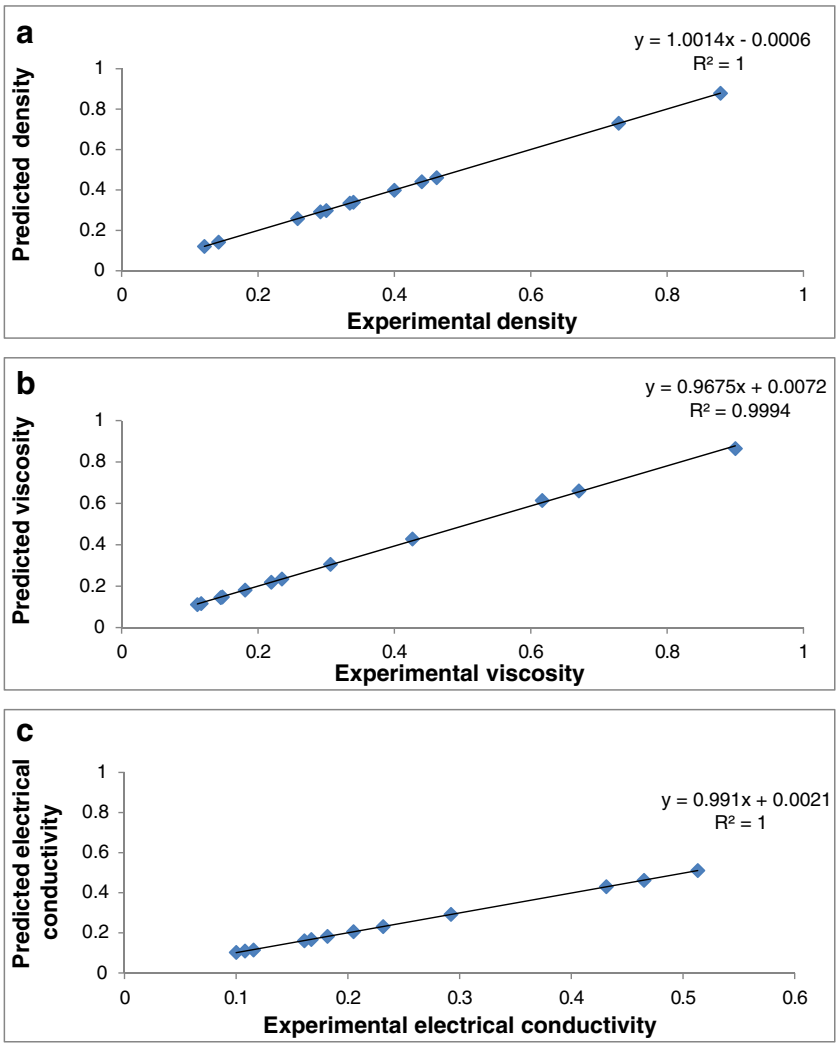

Fig. 4 The predicted values of normalized versus experimental data for **a** density **b** viscosity **c** electrical conductivity and testing set using the ANN model

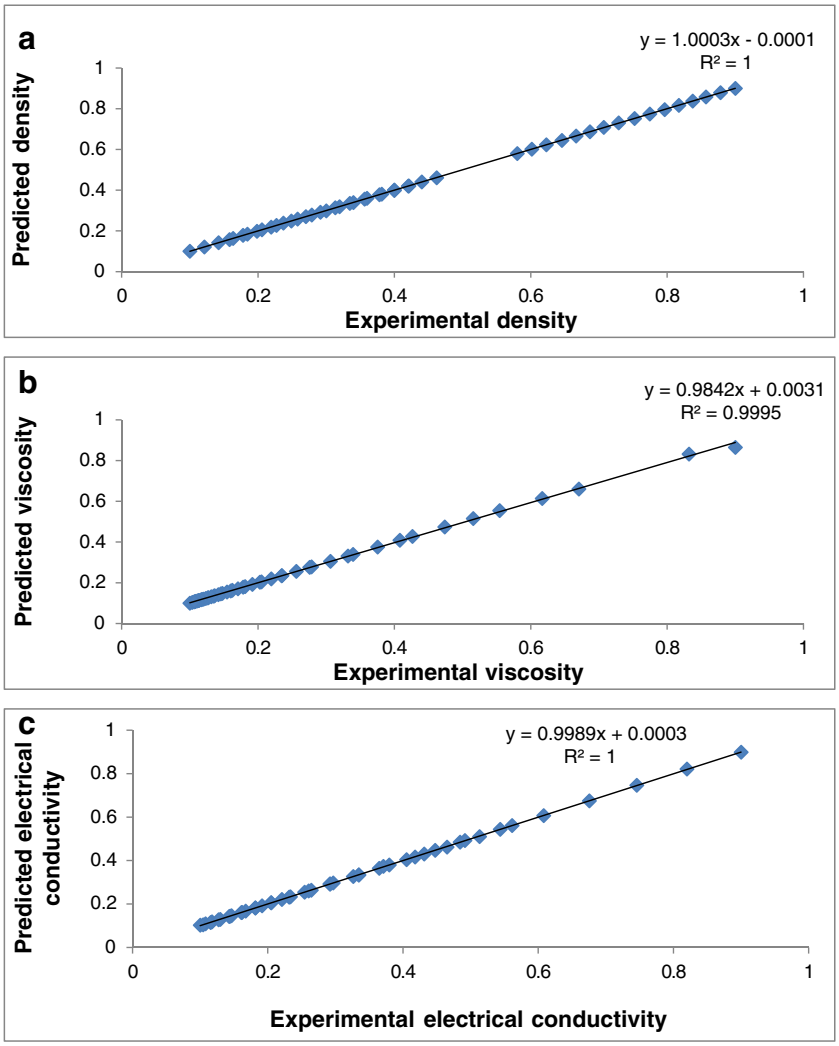

Fig. 5 The predicted values of normalized versus experimental data for **a** density **b** viscosity **c** electrical conductivity and testing set using the ANN model

topologies for prediction of density, viscosity and electrical conductivity, respectively, in training test group and total data, validating the best prediction as the optimal topology. The RMSE and R^2 values for this topology in the test group were found 7. $5714*10^{-7}$, 1.0000, $1.1332*10^{-4}$, 0.9982, $2.2668*10^{-6}$ and 0.9999 for density, viscosity and electrical conductivity, respectively. The Fig. 3 respectively show experimental density, viscosity and electrical conductivity in terms of predicted density, viscosity and electrical conductivity by optimal topology during the training. These figures show a good agreement between experimental and predicted values. Number of tests was used to assess this topology. The Fig. 4 respectively show experimental density, viscosity and electrical conductivity in terms of predicted density, viscosity and electrical conductivity by optimal topology during the test. This topology predicts density, viscosity and electrical conductivity as 1.0000, 0.9994 and 1.0000, respectively. The Fig. 5 respectively show experimental density, viscosity and electrical conductivity in terms of predicted density, viscosity and electrical conductivity by optimal topology for entire the data.

4 Conclusion

An artificial neural network was used in present study to concurrently predict density, viscosity and electrical conductivity of Pyridinium-based hydrophobic ionic liquids. The optimal topology here includes 10 neurons in the hidden layer and is able to concurrently and suitably predict density, viscosity and electrical conductivity. The artificial neural network model shows lower errors and higher precision compared to statistical models while use of ANN is easier and quicker than statistical methods.

Glossary

k	Walden constant
M	Molar mass

S^0	Standard molar entropy
U_{POT}	Lattice energy
ρ	Density
ð	Electrical conductivity
η	Dynamic viscosity
α	Thermal expansion coefficients

References

1. Abbaspour A, Baramakeh L (2005) Simultaneous determination of antimony and bismuth by beta-correction spectrophotometry and an artificial neural network algorithm. Talanta 65:692
2. Agrawal VK, Louis B, Khadikar PV (2010) Prediction of intrinsic solubility of generic drugs using MLR, ANN and SVM analyses. Eur J Med Chem 45:4018
3. Akbari E, Buntat Z, Enzevaee A, Ebrahimi M, Yazdavar AH, Yusof R (2014) Analytical modeling and simulation of I–V characteristics in carbon nanotube based gas sensors using ANN and SVR methods. Chemom Intel Lab 137:173
4. Balabin RM, Lomakina EI, Safieva RZ (2011) Neural network (ANN) approach to biodiesel analysis: analysis of biodiesel density, kinematic viscosity, methanol and water contents using near infrared (NIR) spectroscopy. Fuel 90:2007
5. Bordbar MM, Khajehsharifi H, Solhjoo A (2015) PC-ANN assisted to the determination of Vanadium (IV) ion using an optical sensor based on immobilization of Eriochorome Cyanine R on a triacetylcellulose film. Spectrochim Acta A Mol Biomol Spectrosc 151:225
6. Khajehsharifi H, Bordbar MM (2015) A highly selective chemosensor for detection and determination ofcyanide by using an indicator displacement assay and PC-ANN and itslogic gate behavior. Sensors Actuators 209:1015
7. Ni Y, Xia Z, Kokot S (2011) A kinetic spectrophotometric method for simultaneous determination of phenol and its three derivatives with the aid of artificial neural network. J Hazard Mater 192:722
8. Tenorio-Borroto E, Peñuelas Rivas CG, Vásquez Chagoyán JC, Castañedo N, Prado-Prado FJ, García-Mera X, González-Díaz H (2012) ANN multiplexing model of drugs effect on macrophages; theoretical and flow cytometry study on the cytotoxicity of the anti-microbial drug G1 in spleen. Bioorg Med Chem 20:6181
9. Zamaniyan A, Joda F, Behroozsarand A, Ebrahimi H (2013) Application of artificial neural networks (ANN) for modeling of industrial hydrogen plant. Int J Hydrog Energy 38:6289
10. Lazzari M, Mastragostino M, Pandolfo AG, Ruiz V, Soavi F (2011) J Electrochem Soc 158:A22–A25
11. Rantwijk FV, Sheldon RA (2007) Chem Rev 107:2757–2785
12. Greaves TL, Drummond CJ (2008) Chem Rev 108:206–237
13. Hapiot P, Lagrost C (2008) Chem Rev 108:2238–2264
14. Keskin S, Kayrak D, Akman U (2007) A review of ionic liquids towards supercritical fluid applications. J Supercrit Fluids 43:150
15. Liu QS, Li PP, Welz-Biermann U, Chen J, Liu XX (2013) Density, dynamic viscosity, and electrical conductivity of pyridinium-based hydrophobic ionic liquids. J Chem Thermodyn 66:88
16. Eliassi A, Modarress H, Mansoori A (1998) Density of poly ethylene glycol + water mixtures in the 298.15-328.15 K temperature rang. J Chem Eng Data 43(5):719–721
17. Ensafi A, Khayamian T, Benvidi A, Mirmomtaz E (2006) Simultaneous determination of copper, lead and cadmium by cathodic adsorptive stripping voltammetry using artificial neural network. Anal Chem Acta 561:225
18. Ensafi A, Khayamian T, Atabati M (2002) Simultaneous voltammetric determination of molybdenum and copper by adsorption cathodic differential pulse stripping method using a principal component artificial neural network. Talanta 59:792